# Direct Evidence for a Surface and Bulk Specific Response in the Sum-Frequency Generation Spectrum of the Water Bend Vibration

C. J. Moll,* J. Versluis, and H. J. Bakker
*AMOLF, Ultrafast Spectroscopy, Science Park 104, 1098XG Amsterdam, Netherlands*

(Received 30 March 2021; revised 2 August 2021; accepted 6 August 2021; published 9 September 2021)

We study the bending mode of pure water and charged aqueous surfaces using heterodyne-detected vibrational sum-frequency generation spectroscopy. We observe a low (1626 $cm^{-1}$) and a high (1656 $cm^{-1}$) frequency component that can be unambiguously assigned to an interfacial dipole and a bulk quadrupolar response, respectively. We thus demonstrate that probing the bending mode provides structural and quantitative information on both the surface and the bulk.

DOI: 10.1103/PhysRevLett.127.116001

The structure and dynamics of aqueous interfaces is of high relevance for many different scientific fields [1–9]. Many important chemical and biological processes take place at aqueous interfaces, for instance, molecular recognition at biomembranes, protein folding, and energy conversion and storage [10–15]. The structural properties of the neat water-air interface [16,17] and charged aqueous interfaces have been extensively studied with vibrational sum-frequency generation spectroscopy (VSFG) in the frequency region of the water OH stretch vibrations [11,18–20]. The frequency region of the water bending vibrations has been much less investigated, even though this region can provide unique information on the hydrogen-bond structure, because, in contrast to the stretching mode, the water bending mode is hardly influenced by intermolecular coupling due to its small transition dipole moment [21–23]. Furthermore, there is only one water bending mode per water molecule, thus strongly decreasing the effects of intramolecular coupling on the spectrum. Vinaykin and Benderskii were the first to study the water bending mode of the neat water-air interface with conventional VSFG, for which the response is proportional to the modulo squared of the second-order susceptibility ($|\chi^{(2)}|^2$) [22]. These authors reported the observation of an inhomogeneously broadened line shape centered at 1650 $cm^{-1}$. They assigned the low- and high-frequency wing of this band to weakly hydrogen-bonded water molecules sticking out of the surface and to fully hydrogen-bonded interfacial water molecules, respectively. Furthermore, they found evidence for the presence of a large orientational inhomogeneity [22]. These findings have been confirmed by recent computational studies by Ni and Skinner [21] and Nagata *et al.* [23].

Kundu *et al.* reported the first heterodyne-detected VSFG (HD-VSFG) measurements of the neat water-air interface in the bending mode region [24]. In this technique, the real and imaginary part of the second-order susceptibility $\chi^{(2)}$ are determined. The measured $\mathrm{Im}[\chi^{(2)}]$ showed a single positive peak centered at 1650 $cm^{-1}$. In the same work, it was also reported that charging the interface negative with iodide ions leads to an enhancement of this signal. This observation strongly contrasts with observations in the OH stretching mode region, for which a change of the sign of the band is observed when the surface gets negatively charged [18,20]. The accompanying calculations indicated that the observed $\mathrm{Im}[\chi^{(2)}]$ signal would originate mainly from a quadrupole response from the bulk [24]. In the most recent intensity VSFG measurements of Dutta *et al.* [15], it was found that the interfacial water molecules orient in different directions depending on the charge of the surface, which suggests that the observed signal primarily results from a surface dipolar response. This explanation is consistent with the $|\chi^{(2)}|$ measurements of the group of Bonn and Nagata [25], and thus strongly disagrees with the interpretation of the $\mathrm{Im}[\chi^{(2)}]$ measurements by Kundu *et al.* [24]. Here we perform HD-VSFG measurements to investigate the sum-frequency response of the bending mode of aqueous systems. By measuring the effect of surface charge on the signal, we demonstrate the presence of both a dipolar contribution of the surface and a quadrupolar contribution of the bulk to the signal and we clear up the existing inconsistencies between earlier reports [15,21,22,24,25].

The technique of HD-VSFG has been developed and successfully used by several groups [20,26–28] and is briefly discussed in the Supplemental Material (experimental details) [29]. Here it needs to be mentioned that the water bending mode has a small transition dipole moment and yields to a ~5 times smaller signal than the OH stretching modes. Therefore, the measurement of a clean signal confronts us with several technical challenges. In particular, in the frequency region of the water bending mode, an etaloning effect occurs in the CCD camera, which introduces a systematic modulation on the signal.

 

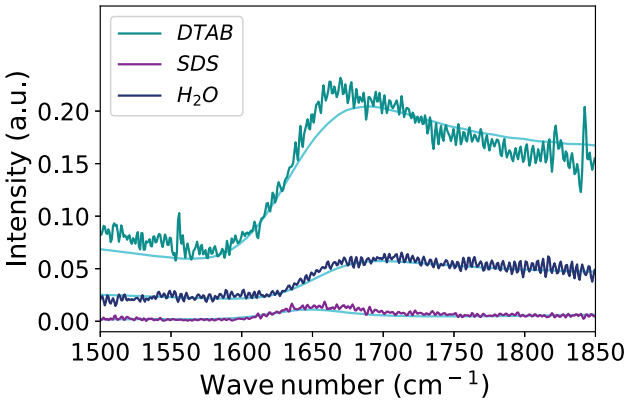


FIG. 1. $|\chi^{(2)}|^2$ spectra of the neat water surface water-air (dark blue), the water-DTAB-air interface (dark cyan) and the water-SDS-air interface (magenta) in the frequency region of the water bend vibration. The concentration of the SDS and DTAB solution is 10 mM. Note that the spectra are not offset with respect to each other; the signal observed for the DTAB solution is much stronger than that of pure water and the SDS solution.

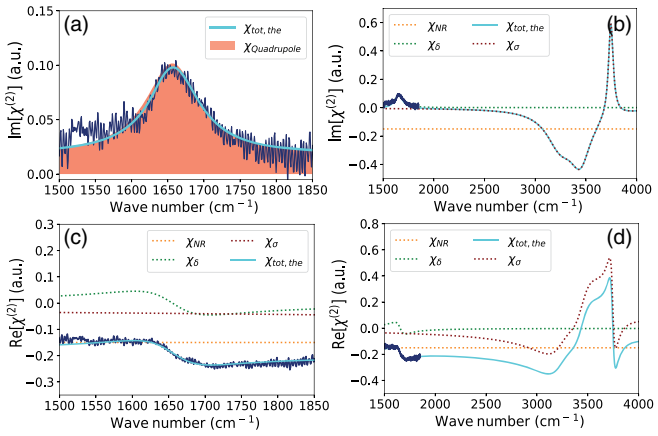


FIG. 2. (a) $\mathrm{Im}[\chi^{(2)}]$ spectrum of neat water (dark blue) in the frequency region of the bending mode. The solid line represents the result of a fit, explained in the text. (b)–(d) Modeled $\mathrm{Im}[\chi^{(2)}]$ and $\mathrm{Re}[\chi^{(2)}]$ spectra of neat water ($\chi_{\mathrm{tot,the}}$, cyan) compared to the experimental data (dark blue). The figures also show the decomposition of the total response $\chi_{\mathrm{tot,the}}$ in different contributions: the nonresonant background $\chi_{\mathrm{NR}}$ (dotted orange), the bending mode response $\chi_{\delta}$ (dotted green), and the response of the OH stretch vibrations $\chi_{\sigma}$ (dotted red).

A detailed explanation of the measurement procedure to remove this systematic modulation and to detect high-quality data in the region of the water bending mode can be found in the Supplemental Material (Noise reduction and measurement procedure) [29].

In Fig. 1 we present $|\chi^{(2)}|^2$ (intensity VSFG) spectra of the neat water surface water-air (dark blue), the water-dodecyltrimethylammonium bromide (DTAB)-air interface (dark cyan), and the water-sodium dodecyl sulfate (SDS)-air interface (magenta) in the frequency region of the water bend vibration. For pure water we observe that the $|\chi^{(2)}|^2$ spectrum has the shape of a step function, in agreement with previous findings [22]. The addition of a charged surfactant leads to strong changes of the response. Adding the positively charged DTAB leads to an enhancement and a redshift of the response; adding the negatively charged SDS leads to a redshift of the maximum of the sum-frequency generation (SFG) intensity. These findings are in line with previous intensity VSFG measurements performed by Dutta *et al.* [15]. The solid cyan curves in Fig. 1 are the result of model calculations, as described in the text below and in the Supplemental Material [29].

In Fig. 2(a) the experimental $\mathrm{Im}[\chi^{(2)}]$ spectra of neat water (dark blue) in the frequency region of the water bend vibration is presented. We observe a symmetric positive peak centered at 1656 $\mathrm{cm}^{-1}$ that we assign to the water bending mode. The observed spectrum agrees with previous HD-VSFG measurements of Kundu *et al.* [24]. We find that this $\mathrm{Im}[\chi^{(2)}]$ response can be fitted well with a single Lorentzian curve (cyan). In Fig. 2(b) we show a comparison of the calculated $\mathrm{Im}[\chi^{(2)}]$ spectrum of neat water over a broad frequency region (cyan) combined with the experimental data (dark blue) in the frequency region of the water bending mode. In addition to the water bending mode, the model includes the resonances of the OH stretch vibrations of hydrogen-bonded and non-hydrogen-bonded water molecules (red dotted line, $\chi_{\sigma,\mathrm{OH}}$). The OH stretch band of the hydrogen-bonded water molecules is modeled with two Lorentzian curves with maxima at 3250 and 3450 $\mathrm{cm}^{-1}$, and the response of the non-hydrogen-bonded water molecules is modeled with a single Lorentzian centered at 3700 $\mathrm{cm}^{-1}$. In addition to the resonances in the stretching mode region, we included a frequency-independent nonresonant background $\chi_{\mathrm{NR}}$ (orange dotted). The comparison of the model and the experimental data shows that the resonances of the OH stretch band have a negligible influence on the observed $\mathrm{Im}[\chi^{(2)}]$ in the bending mode region. However, the $\mathrm{Re}[\chi^{(2)}]$ in the bending mode region does show significant contributions from both the different OH stretch vibrations $\chi_{\sigma,\mathrm{OH}}$ and the nonresonant background $\chi_{\mathrm{NR}}$, as illustrated in Figs. 2(c) and 2(d). The low-frequency wing of the real response of the stretching band (red dotted) adds a negative value to the real part of the response of the bending mode $\chi_{\delta}$ (green dotted). In Fig. 2(d) we show the $\mathrm{Re}[\chi^{(2)}]$ over a broad frequency range. This figure clearly shows that the $\chi_{\sigma}$ contribution also induces a slight tilt of the total $\mathrm{Re}[\chi^{(2)}]$ in the frequency region of the bending mode. From the analysis of Fig. 2 it is clear that the observed step in the intensity SFG spectrum of pure water of Fig. 1 can be well explained from the interference with the stretch vibrations. The $\mathrm{Re}[\chi^{(2)}_{\sigma}]$ of the stretch vibrations compensates the positive $\mathrm{Re}[\chi^{(2)}_{\delta}]$ of the bending vibration at frequencies $<1650$ $\mathrm{cm}^{-1}$ and enhances the negative $\mathrm{Re}[\chi^{(2)}_{\delta}]$ of the

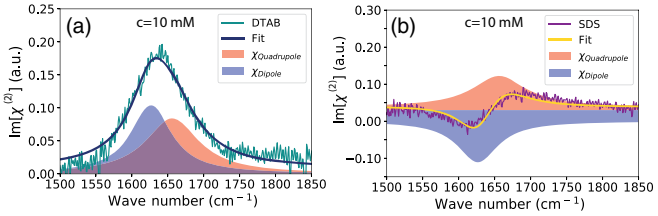


FIG. 3. Spectral decomposition of the $\mathrm{Im}[\chi^{(2)}]$ spectra of (a) the water-DTAB-air interface (dark cyan) and (b) the water-SDS-air interface (magenta), each modeled with two Lorentzian-shaped spectral components.The two Lorentzian-shaped components are assigned to the quadrupolar contribution of the bulk (red, centered at 1656 $\mathrm{cm}^{-1}$) and to the surface dipolar contribution (blue, centered at 1626 $\mathrm{cm}^{-1}$) of the water bending mode.

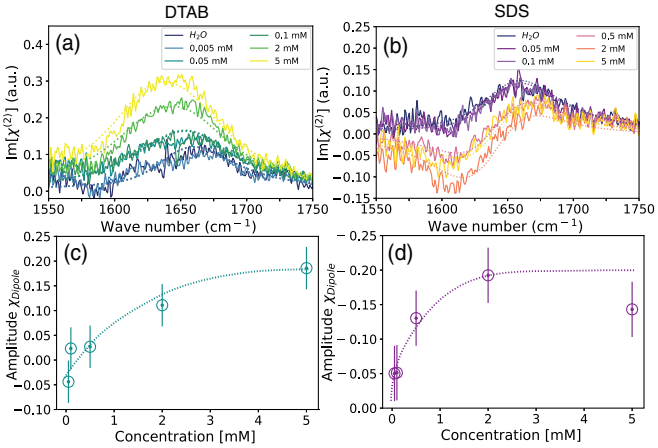


FIG. 4. The $\mathrm{Im}[\chi^{(2)}]$ spectra of the (a) water-DTAB-air and (b) water-SDS-air interfaces at different concentrations in the range of 0.05–5 mM including fits presented with dashed lines. (c),(d) The absolute amplitude of the dipole contribution extracted from the fitting procedure in respect to the concentration of (c) DTAB and (d) SDS.

bending vibration at frequencies >1650 $\mathrm{cm}^{-1}$. As a result, the total intensity ($|\chi^{(2)}|^2$) shows a steplike shape.

In Fig. 3, we present experimental $\mathrm{Im}[\chi^{(2)}]$ spectra of the water-DTAB-air interface (dark cyan) and the water-SDS-air interface (magenta) in the frequency region of the water bend vibration. The $\mathrm{Im}[\chi^{(2)}]$ spectrum of the water-DTAB-air interface shows a positive band centered at 1640 $\mathrm{cm}^{-1}$. This band is stronger, broader, and somewhat redshifted in comparison to the $\mathrm{Im}[\chi^{(2)}]$ spectrum of the water-air interface. The $\mathrm{Im}[\chi^{(2)}]$ spectrum of the water-SDS-air interface shows a clear negative feature at lower frequencies. At this point, it should be noted that we can exclude phase distortions in the HD-VSFG spectra, as the electric double layer has a thickness <10 nm for ionic strengths >1 mM [40–42]. The spectra observed for water-DTAB-air and water-SDS-air interfaces can be well explained from the presence of an additional low-frequency band in the $\mathrm{Im}[\chi^{(2)}]$ spectra that is negligibly present for the neat water-air interface and that has a different sign for the water-DTAB-air and the water-SDS-air interfaces. To substantiate that the lower-frequency band depends on the sign of the surface charge, we also performed measurements with a different negatively charged surfactant sodium monododecyl phosphate (Supplemental Material Fig. S3 [29]). These measurements also show the presence of a negative band centered at 1626 $\mathrm{cm}^{-1}$, thus confirming that this band results from the bending mode of water and that its sign is determined by the sign of the surface charge. To quantify the different contributions to the $\mathrm{Im}[\chi^{(2)}]$ spectra, we decompose the spectra observed for the water-DTAB-air interface and the water-SDS-air interface into Lorentzian-shaped bands centered at 1656 (blue) and 1626 $\mathrm{cm}^{-1}$ (red). The band at 1656 $\mathrm{cm}^{-1}$ does not depend on the charge of the surface and is assigned to the quadrupolar response of the bulk. This assignment is consistent with the notion that the quadrupolar contribution of the water bending mode does not depend on the orientation of the water molecules and is thus not strongly affected by the surface electric field [43]. The sign and amplitude of the 1626 $\mathrm{cm}^{-1}$ band are determined by the charge at the surface and can therefore be assigned to a dipolar surface contribution. This assignment is further supported by studying the effect of adding 0.5 M NaCl to the water-DTAB and the water-SDS solutions. The addition of salt leads to screening of the electric field of the charged surfactants. We observe that the addition of salt leads to a vanishing of the 1626 $\mathrm{cm}^{-1}$ band (Supplemental Material Fig. S4 [29]).

For the positively charged DTAB-air surface the interfacial water molecules are oriented with their hydrogen atoms toward the bulk. For the stretch vibration, this orientation leads to a negative contribution to $\mathrm{Im}[\chi^{(2)}]$, because for the stretch vibration the dipole and the polarizability have the same dependence on the phase of the stretch vibration (when the hydrogen atoms move away from the oxygen atom, the dipole moment increases and the size and polarizability of the water molecules also increase). For the bending vibration, the dipole moment and polarizability have an opposite dependence on the phase of the bending vibration (when the atoms move together, the dipole moment increases, while the size and polarizability of the water molecule decreases). As a result, the surface dipolar contribution to the $\mathrm{Im}[\chi^{(2)}]$ of the bending mode is positive for water molecules with their hydrogen atoms oriented toward the bulk and negative for water molecules that have their hydrogen atoms oriented toward the surface.

For neat water, we find that the experimental data can be well described with a single Lorentzian line that only represents the quadrupolar contribution of the bulk (Fig. 2). In our fitting procedure for the water-DTAB-air and water-SDS-air (10 mM) interfaces presented in Figs. 3(a) and 3(b), we use the same description for the quadrupolar contribution. In the Supplemental Material [29] we show

the measured $\mathrm{Re}[\chi^{(2)}]$ responses of the water-DTAB-air interface and the water-SDS-air interface and the decomposition of the $\mathrm{Im}[\chi^{(2)}]$ and $\mathrm{Re}[\chi^{(2)}]$ spectra (Supplemental Material Figs. 5 and 6), as was done for the neat water-air interface, which was shown in Fig. 2. In this analysis, we include the interference effect between the quadrupolar bulk and dipolar interface responses of the bending mode and the interference effect between the water bending mode responses and the response of the OH stretch vibrations and the nonresonant background response. We find that for the water-DTAB-air interface and the water-SDS-air interface, the $\mathrm{Re}[\chi^{(2)}]$ response and the intensity spectrum ($\sim|\chi^{(2)}|^2$) are strongly affected by the interference with the response of the OH stretch vibrations, as was the case for neat water.

In Figs. 4(a) and 4(b), respectively, we present the $\mathrm{Im}[\chi^{(2)}]$ spectra of water-DTAB-air and water-SDS-air interfaces at different concentrations in the range of 0–5 mM. For the water-DTAB-air interface we observe that the positive peak centered at 1656 $\mathrm{cm}^{-1}$ assigned to the water bending mode is increasing with increasing DTAB concentration. Furthermore, we observe a broadening and a slight redshift of the $\mathrm{Im}[\chi^{(2)}]$ spectra. Increasing the SDS concentration leads to an ingrowth of a negative peak at lower frequencies. These observations confirm the assignment of the band at 1626 $\mathrm{cm}^{-1}$ to a surface dipolar contribution. In the case of DTAB, the positive surface charge is increasing with increasing concentration, thus causing an enhanced ordering of the interfacial water molecules with their hydrogen atoms toward the bulk, which leads to an increase of a positive dipolar band at 1626 $\mathrm{cm}^{-1}$. The increase of the concentration of SDS increases the negative charge density at the surface, thereby inducing an enhanced orientation of the water molecules with their hydrogen atoms toward the surface and thus to an increase of a negative dipolar contribution at 1626 $\mathrm{cm}^{-1}$. The concentration-dependent increase of the dipolar contribution of the water bending mode is also observed for the OH stretch vibration of aqueous solutions of DTAB and SDS (Supplemental Material Fig. S7 [29]).

To quantify the results, we decompose the responses measured at different concentrations of DTAB and SDS in two Lorentzian bands centered at 1626 and 1656 $\mathrm{cm}^{-1}$ for the dipole and quadrupole contribution, respectively. As the quadrupolar contribution is not expected to depend on the orientation of the water molecules, we keep the quadrupolar contribution constant at all concentrations. We also keep the width of the dipolar contribution constant, and we only allow the amplitude of this contribution to change with the surfactant concentration. The fits are shown in Figs. 4(a) and 4(b) with dashed lines. The decompositions for the different concentrations are presented in the Supplemental Material (Figs. 8 and 9). In Figs. 4(c) and 4(d), we present the amplitude of the dipolar band extracted from the fitting procedure as a function of the surfactant concentration. For both DTAB and SDS, the amplitude of the dipolar band increases nonlinearly with concentration, showing saturation behavior at a bulk concentration of a few millimolar. This saturation behavior can be explained from the saturation of the surface density of surfactant molecules, the resulting decrease of the water density at the surface, and the enhanced screening effect of the counter ions of the surfactant molecules. A similar saturation effect is observed for the OH stretching mode of water (Supplemental Material Fig. S7 [29]). The combination of these effects can even lead to a decrease of the dipolar response at higher SDS concentrations. From the fitting procedure, we find that at a surfactant concentration of 10 mM the absolute ratio of the amplitudes of the dipolar interfacial and the quadrupolar bulk contribution is 1∶0.7, both for the water-DTAB-air interface and the water-SDS-air interface. It is also seen that at zero surfactant concentration the dipolar contribution is negligible.

Recently Ahmed *et al.* [44] reported HD-VSFG measurements of water with charged surfactants and lipid monolayer-water interfaces in which they did not find evidence for an interfacial dipole contribution of the water bending mode. Their $\mathrm{Im}[\chi^{(2)}]$ spectra show a positive band, independent of the sign of the charge of the headgroup. Therefore, Ahmed *et al.* argued that the $\mathrm{Im}[\chi^{(2)}]$ response of the water bending mode arises only from a quadrupolar response, even for charged surfaces [44]. At first sight this finding appears to disagree with the results of Fig. 3. However, the measurements of Ahmed *et al.* were performed with a surfactant concentration of only 0.1 mM, while the measurements shown in Fig. 3 are performed with a surfactant concentration of 10 mM. As is clearly illustrated in Fig. 4, for a surfactant concentration of 0.1 mM, the dipolar contribution is negligibly small. To detect the dipolar contribution of the OH bending mode, a sufficiently high surface charge density is needed. The absence of a dipolar contribution in the SFG spectrum of the water bending mode for a 2.1 M NaI solution in the work of Kundu *et al.* [24] can thus be explained from the relatively low negative surface charge density of NaI solutions in comparison to SDS solutions.

An interesting observation is that the dipolar contribution has a significantly lower frequency than the quadrupolar contribution. The lower frequency of the dipolar contribution indicates that the hydrogen bonds of the contributing water molecules are weaker than those of the water molecules giving rise to the quadrupolar contribution [22]. This finding agrees with the fact that the molecules giving rise to the quadrupolar contribution are predominantly located in the bulk of the liquid, whereas the molecules giving rise to the dipolar contribution will be located at the surface.

In summary, we performed HD-VSFG measurements of pure water and of aqueous solutions of ionic surfactants. We find that the $\mathrm{Im}[\chi^{(2)}]$ response in the frequency region of the bending mode of water is strongly affected by the

interference with the low-frequency wing of the OH stretch vibrations of water. By comparing the measured $\mathrm{Im}[\chi^{(2)}]$ spectra of differently charged water surfaces, we demonstrate the presence of a surface specific dipolar response of the water bending mode centered at 1626 $\mathrm{cm}^{-1}$. This response changes sign when the sign of the surface charge changes and increases with increasing surface charge, i.e., increasing concentration of ionic surfactant. In addition to this dipolar surface contribution, the bending mode of water shows a quadrupolar bulk contribution centered at 1656 $\mathrm{cm}^{-1}$. This contribution is not surface charge dependent and dominates the $\mathrm{Im}[\chi^{(2)}]$ response of neat water in the frequency region of the bending mode. The water bending vibrations form an excellent probe of the (hydrogen-bonded) environment of the water molecule, as they are much less effected by intra- and intermolecular couplings than the stretch vibrations. Therefore, small changes in frequency and amplitude of the bending mode spectrum can be directly connected to changes in the environment of the water molecules. We thus demonstrate that HD-VSFG involving the bending mode of the water molecules can provide important information on the hydrogen-bond structure of both the surface and bulk of aqueous solutions.

This work is part of the research program of the Netherlands Organization for Scientific Research (NWO) and was performed at the research institute AMOLF. This project has received funding from the European Research Council (ERC) under the European Unions Horizon 2020 Research and Innovation Program (Grant Agreement No. 694386).

*cmoll@amolf.nl

[1] S. Nihonyanagi, S. Yamaguchi, and T. Tahara, Ultrafast dynamics at water interfaces studied by vibrational sum frequency generation spectroscopy, Chem. Rev. **117**, 10665 (2017).

[2] H. Koinuma, A. Ohtomo, H. Y. Hwang, S. M. Sze, H.-S. S. Devices, D. A. Muller, J. L. Grazul, S. Okamoto, A. J. Millis, J. Mannhart, J. G. Bednorz, K. A. Mu, D. G. Schlom, C. H. Ahn, N. Nakagawa, H. L. Stormer, O. N. Tufte, P. W. Chapman, and E. Williams, Ultrafast dynamics at water interfaces, Science **313**, 1945 (2006).

[3] J. D. Cyran, E. H. G. Backus, Y. Nagata, and M. Bonn, Structure from dynamics: Vibrational dynamics of interfacial water as a probe of aqueous heterogeneity, J. Phys. Chem. B **122**, 3667 (2018).

[4] S. Strazdaite, J. Versluis, E. H. G. Backus, and H. J. Bakker, Enhanced ordering of water at hydrophobic surfaces, J. Chem. Phys. **140**, 054711 (2014).

[5] X. Chen, T. Yang, S. Kataoka, and P. S. Cremer, Specific ion effects on interfacial water structure near macromolecules, J. Am. Chem. Soc. **129**, 12272 (2007).

[6] W. Xiong, J. E. Laaser, R. D. Mehlenbacher, and M. T. Zanni, Adding a dimension to the infrared spectra of interfaces using heterodyne detected 2D sum-frequency generation (HD 2D SFG) spectroscopy, Proc. Natl. Acad. Sci. U.S.A. **108**, 20902 (2011).

[7] C.-S. Hsieh, M. Okuno, J. Hunger, E. H. G. Backus, Y. Nagata, and M. Bonn, Aqueous heterogeneity at the air/water interface revealed by 2D-HD-SFG spectroscopy, Angew. Chem., Int. Ed. Engl. **53**, 8146 (2014).

[8] E. Tyrode, S. Sengupta, and A. Sthoer, Identifying eigen-like hydrated protons at negatively charged interfaces, Nat. Commun. **11**, 493 (2020).

[9] P. C. Singh, S. Nihonyanagi, S. Yamaguchi, and T. Tahara, Interfacial water in the vicinity of a positively charged interface studied by steady-state and time-resolved heterodyne-detected vibrational sum frequency generation, J. Chem. Phys. **141**, 18C527 (2014).

[10] S. Strazdaite, K. Meister, and H. J. Bakker, Orientation of polar molecules near charged protein interfaces, Phys. Chem. Chem. Phys. **18**, 7414 (2016).

[11] Y. C. Wen, S. Zha, X. Liu, S. Yang, P. Guo, G. Shi, H. Fang, Y. R. Shen, and C. Tian, Unveiling Microscopic Structures of Charged Water Interfaces by Surface-Specific Vibrational Spectroscopy, Phys. Rev. Lett. **116**, 016101 (2016).

[12] P. Lo Nostro and B. W. Ninham, Hofmeister phenomena: An update on ion specificity in biology, Chem. Rev. **112**, 2286 (2012).

[13] L. Zhang, Y. Yang, Y. T. Kao, L. Wang, and D. Zhong, Protein hydration dynamics and molecular mechanism of coupled water-protein fluctuations, J. Am. Chem. Soc. **131**, 10677 (2009).

[14] M. F. Toney, J. N. Howard, J. Richer, G. L. Borges, J. G. Gordon, and O. R. Melroy, D. G. Wiesler, D. Yee, and L. B. Sorensen, Voltage-dependent ordering of water molecules at an electrode–electrolyte interface, Nature (London) **368**, 444 (1994).

[15] C. Dutta, M. Mammetkuliyev, and A. V. Benderskii, Re-orientation of water molecules in response to surface charge at surfactant interfaces, J. Chem. Phys. **151**, 034703 (2019).

[16] Q. Du, R. Superfine, E. Freysz, and Y. R. Shen, Vibrational Spectroscopy of Water at the Vapor/Water Interface, Phys. Rev. Lett. **70**, 2313 (1993).

[17] C. J. Tainter, Y. Ni, L. Shi, and J. L. Skinner, Hydrogen bonding and oh-stretch spectroscopy in water: Hexamer (cage), liquid surface, liquid, and ice, J. Phys. Chem. Lett. **4**, 12 (2013).

[18] C. Tian, S. J. Byrnes, H. L. Han, and Y. R. Shen, Surface propensities of atmospherically relevant ions in salt solutions revealed by phase-sensitive sum frequency vibrational spectroscopy, J. Phys. Chem. Lett. **2**, 1946 (2011).

[19] C. S. Tian and Y. R. Shen, Structure and charging of hydrophobic material/water interfaces studied by phase-sensitive sum-frequency vibrational spectroscopy, Proc. Natl. Acad. Sci. U.S.A. **106**, 15148 (2009).

[20] S. Nihonyanagi, S. Yamaguchi, and T. Tahara, Direct evidence for orientational flip-flop of water molecules at charged interfaces: A heterodyne-detected vibrational sum frequency generation study, J. Chem. Phys. **130**, 204704 (2009).

[21] Y. Ni and J. L. Skinner, IR and SFG vibrational spectroscopy of the water bend in the bulk liquid and at the liquid-vapor interface, respectively, J. Chem. Phys. **143**, 014502 (2015).

[22] M. Vinaykin and A. V. Benderskii, Vibrational sum-frequency spectrum of the water bend at the air/water interface, J. Phys. Chem. Lett. **3**, 3348 (2012).
[23] Y. Nagata, C. S. Hsieh, T. Hasegawa, J. Voll, E. H. Backus, and M. Bonn, Water bending mode at the water-vapor interface probed by sum-frequency generation spectroscopy: A combined molecular dynamics simulation and experimental study, J. Phys. Chem. Lett. **4**, 1872 (2013).
[24] A. Kundu, S. Tanaka, T. Ishiyama, M. Ahmed, K. I. Inoue, S. Nihonyanagi, H. Sawai, S. Yamaguchi, A. Morita, and T. Tahara, Bend vibration of surface water investigated by heterodyne-detected sum frequency generation and theoretical study: Dominant role of quadrupole, J. Phys. Chem. Lett. **7**, 2597 (2016).
[25] T. Seki, S. Sun, K. Zhong, C. C. Yu, K. MacHel, L. B. Dreier, E. H. Backus, M. Bonn, and Y. Nagata, Unveiling heterogeneity of interfacial water through the water bending mode, J. Phys. Chem. Lett. **10**, 6936 (2019).
[26] V. Ostroverkhov, G. A. Waychunas, and Y. R. Shen, New Information on Water Interfacial Structure Revealed by Phase-Sensitive Surface Spectroscopy, Phys. Rev. Lett. **94**, 046102 (2005).
[27] S. Yamaguchi and T. Tahara, Heterodyne-detected electronic sum frequency generation: "Up" versus "down" alignment of interfacial molecules, J. Chem. Phys. **129**, 101102 (2008).
[28] C. J. Moll, K. Meister, J. Kirschner, and H. J. Bakker, Surface structure of solutions of poly(vinyl alcohol) in water, J. Phys. Chem. B **122**, 10722 (2018).
[29] See Supplemental Material at http://link.aps.org/supplemental/10.1103/PhysRevLett.127.116001 for the experimental details, noise reduction and measurement procedure, quadrupolar contribution of the water bending mode, and supporting Figs. 1–9, which includes [30–39].
[30] Y. R. Shen, Phase-sensitive sum-frequency spectroscopy, Annu. Rev. Phys. Chem. **64**, 129 (2013).
[31] R. E. Pool, J. Versluis, E. H. Backus, and M. Bonn, Comparative study of direct and phase-specific vibrational sum-frequency generation spectroscopy: Advantages and limitations, J. Phys. Chem. B **115**, 15362 (2011).
[32] S. Nihonyanagi, S. Yamaguchi, and T. Tahara, Counterion effect on interfacial water at charged interfaces and its relevance to the Hofmeister series, J. Am. Chem. Soc. **136**, 6155 (2014).
[33] M. M. Sartin, W. Sung, S. Nihonyanagi, and T. Tahara, Molecular mechanism of charge inversion revealed by polar orientation of interfacial water molecules: A heterodyne-detected vibrational sum frequency generation study, J. Chem. Phys. **149**, 024703 (2018).
[34] L. B. Dreier, Y. Nagata, H. Lutz, G. Gonella, J. Hunger, E. H. Backus, and M. Bonn, Saturation of charge-induced water alignment at model membrane surfaces, Sci. Adv. **4**, eaap7415 (2018).
[35] K. Shiratori and A. Morita, Theory of quadrupole contributions from interface and bulk in second-order optical processes, Bull. Chem. Soc. Jpn. **85**, 1061 (2012).
[36] K. Matsuzaki, S. Nihonyanagi, S. Yamaguchi, T. Nagata, and T. Tahara, Vibrational sum frequency generation by the quadrupolar mechanism at the nonpolar benzene/air interface, J. Phys. Chem. Lett. **4**, 1654 (2013).
[37] W. Mori, L. Wang, Y. Sato, and A. Morita, Development of quadrupole susceptibility automatic calculator in sum frequency generation spectroscopy and application to methyl CH vibrations, J. Chem. Phys. **153**, 174705 (2020).
[38] S. Yamaguchi, K. Shiratori, A. Morita, and T. Tahara, Electric quadrupole contribution to the nonresonant background of sum frequency generation at air/liquid interfaces, J. Chem. Phys. **134**, 184705 (2011).
[39] Y. R. Shen, Revisiting the basic theory of sum-frequency generation, J. Chem. Phys. **153**, 180901 (2020).
[40] D. E. Gragson and G. L. Richmond, Investigations of the structure and hydrogen bonding of water molecules at liquid surfaces by vibrational sum frequency spectroscopy, J. Phys. Chem. B **102**, 3847 (1998).
[41] P. E. Ohno, H. F. Wang, F. Paesani, J. L. Skinner, and F. M. Geiger, Second-order vibrational lineshapes from the air/water interface, J. Phys. Chem. A **122**, 4457 (2018).
[42] P. E. Ohno, H. F. Wang, and F. M. Geiger, Second-order spectral lineshapes from charged interfaces, Nat. Commun. **8**, 1 (2017).
[43] A. Morita, *Theory of Sum Frequency Generation Spectroscopy* (Springer, New York, 2018).
[44] M. Ahmed, S. Nihonyanagi, A. Kundu, S. Yamaguchi, and T. Tahara, Resolving the controversy over dipole versus quadrupole mechanism of bend vibration of water in vibrational sum frequency generation spectra, J. Phys. Chem. Lett., **11**, 9123 (2020).